Time and magnetic field dependent magnetic order in $Ca_3Co_2O_6$ revealed by resonant x-ray scattering

S. M. Yusuf,[1,2,*,†] A. Jain,[1,2,*] A. K. Bera,[1,2] S. S. Meena,[1] D. K. Shukla,[3,‡] and J. Strempfer[3,§]

[1]*Solid State Physics Division, Bhabha Atomic Research Centre, Mumbai 400 085, India*

[2]*Homi Bhabha National Institute, Anushaktinagar, Mumbai 400 094, India*

[3]*Deutsches Elektronen-Synchrotron (DESY), 22607 Hamburg, Germany*

(Received 24 May 2022; revised 18 March 2023; accepted 5 April 2023; published 3 May 2023)

The observation of time dependent magnetic order in the spin-chain compound $Ca_3Co_2O_6$, a promising candidate for showing out-of-equilibrium magnetization behavior, has received tremendous attention for over a decade. The present study uses resonant magnetic scattering close to the cobalt K-absorption edge to probe directly the time, temperature, and magnetic field dependence of the magnetic order in a $Ca_3Co_2O_6$ single crystal. Energy dependences of the magnetic signal and their simulation suggest that the resonant x-ray scattering (RXS) signal at the pre-edge contains contributions only from quadrupole (E2E2) and dipolar-quadrupolar (E1E2) transition processes. Interestingly, the flat intensity variation as a function of azimuthal angle over a wide angular range cannot be explained by considering the ordering of magnetic dipole moments alone. The observed magnetic order below the Néel temperature T_N in the present RXS study differs significantly from the reported neutron diffraction results, indicating possible contributions from high-order moments in addition to the magnetic dipole moment.

DOI: 10.1103/PhysRevB.107.184406

I. INTRODUCTION

Interest in the investigation of nonequilibrium phases of matter and their phase transitions via a change in the thermodynamic parameter in the field of nonequilibrium physics ranges from quantum spin systems to cosmological phenomena [1–5]. The timescales of nonequilibrium phase transitions vary from picoseconds to millions of years. Tracking the nonequilibrium phases in quantum spin systems requires techniques with a time resolution on the order of picoseconds to a couple of minutes, depending upon the dynamics.

Relaxation dynamics of magnetic order in Ising magnets has recently attracted a lot of attention because it plays a crucial role in the determination of the dynamic susceptibility as well as nonequilibrium thermodynamics. About a decade ago, a magnetic order-order transition with a timescale of several hours was found in $Ca_3Co_2O_6$, a system having ferromagnetic Ising spin chains coupled by weak antiferromagnetic interchain interactions [6–11]. Its crystal structure (space group R-3c) contains spin chains (Fig. 1) made up of alternating face-sharing CoO_6 octahedra (OCT) and CoO_6 trigonal prisms (TP) running along the crystallographic c-axis and arranged on a triangular lattice in the a-b plane [12–43]. Due to different crystalline electric fields, the Co^{3+} ions (d^6) at the TP and OCT sites are in the high-spin ($S = 2$) and low-spin ($S = 0$) states, respectively [16,17]. Besides, the Co^{3+} (TP) ions have very strong Ising-like magnetic anisotropy (spin along the c-axis) [42]. DC magnetization measurements [11,15] as well as x-ray and neutron diffraction (ND) studies [18,25,30] show various time dependent and irreversible features, the origin of which has not been fully understood thus far.

ND studies have confirmed the presence of long-range magnetic (dipole) order in $Ca_3Co_2O_6$ below 25 K (T_N). Evidence of higher order moments (like quadrupole) has not been reported thus far, probably because they cannot be detected directly through ND. In this work, we report systematic resonant x-ray scattering (RXS) studies to probe the time and magnetic field dependencies of the magnetic order in $Ca_3Co_2O_6$. Our RXS results establish the presence of an ordered magnetic dipole moment on the Co^{3+} (TP) ions, but also reveal the possible presence of higher order moments. Contrary to previous ND studies [18,25,30], our RXS measurements show a field dependent reversible behavior.

II. EXPERIMENTAL

$Ca_3Co_2O_6$ single crystals were grown in a molten K_2CO_3 flux, as described in Ref. [25]. The RXS experiments were carried out at the cobalt K-edge at beamline P09 at the PETRA III synchrotron radiation source at DESY, Hamburg, Germany. For the RXS experiments under applied magnetic fields along the c-axis, π-polarized incident x rays were used. Experiments were performed in horizontal scattering geometry with ($h\,k\,0$) oriented in the horizontal scattering plane. For the magnetic (7 0 0) reflection, the data were recorded in both, the π-π' and the π-σ' polarization channels. Rotation of the

*These authors contributed equally to this work.

†smyusuf@barc.gov.in

‡Present address: UGC-DAE Consortium for Scientific Research, Khandwa Road, Indore 01, India.

§Present address: Argonne National Laboratory, Lemont, IL, USA.

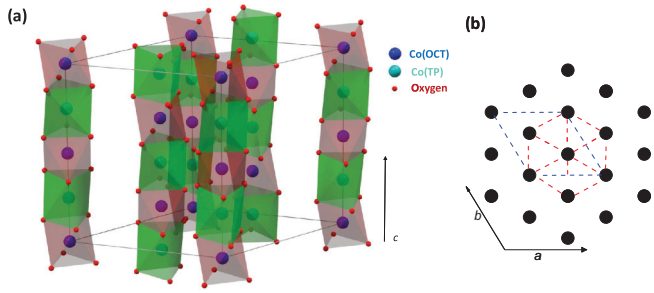

FIG. 1. The crystal structure of $Ca_3Co_2O_6$. (a) A perspective view showing spin chains, made up of alternating face-sharing CoO_6 octahedra and CoO_6 trigonal prisms, running along the crystallographic c-axis. The calcium cations are not shown for clarity. (b) Lattice projected along the c-axis showing a triangular arrangement of spin chains. Each filled circle represents a chain.

sample with respect to the scattering vector was not possible in this configuration; therefore, the azimuthal angle (Ψ) dependence of the scattering intensity of the magnetic reflection could not be measured. This was instead done in another experimental setup on the same beam PX09 line without an applied magnetic field using a diffractometer operating in the vertical scattering geometry with $\sigma-$polarized incident x rays. The Ψ dependence of the scattered intensity of the magnetic (3 2 0) reflection, having the same magnetic ordering vector as the (7 0 0) reflection, was recorded in the $\sigma-\pi'$ channel. For both horizontal and vertical scattering geometries, a pyrolytic-graphite (PG) (6 0 0) crystal was used as polarization analyzer. The dc magnetization measurements were carried out using a commercial magnetometer (Cryogenic Co. Ltd., UK).

III. RESULTS AND DISCUSSION

In Fig. 2(a)–2(f), we show the time evolution of the magnetic (7 0 0) reflection, at 5, 10, and 17 K under zero-applied magnetic fields in the π-π' channel. At 5 and 10 K, the intensity increases with time for up to ∼90 min and afterward it becomes time independent. However, at 17 K, the intensity decreases with time for up to 100 min. Moreover, a significant increase in the peak width [full width at half maximum (FWHM)] with time is observed at 5 and 10 K [Fig. 2(d)–2(f)], indicating that the magnetic correlation length decreases with time. The observed time dependent behavior in our RXS study differs significantly from the one reported in the literature from ND measurements [8], where no time dependency was observed at 17 K. This can be attributed to ND measurements being considerably slower than the RXS measurements and the magnetic correlation length not changing at this temperature [Fig. 2(d)]. Moreover, contrary to the observed increase in intensity here, ND studies show a decrease in intensity of the antiferromagnetic (1 0 0) reflection with time for $8 \leqslant T \leqslant 10$ K [8]. The unusual temperature dependent behavior of the RXS intensity with a maximum at ∼18 K [inset, Fig. 2(c)] agrees with the results reported in the literature [7,8,25,30]. To understand the origin of the observed unusual time dependent behavior of the magnetic order, we measured the (7 0 0) peak at 2 K and 10 K, in the π-σ' channel, where a weak but finite intensity is clearly visible

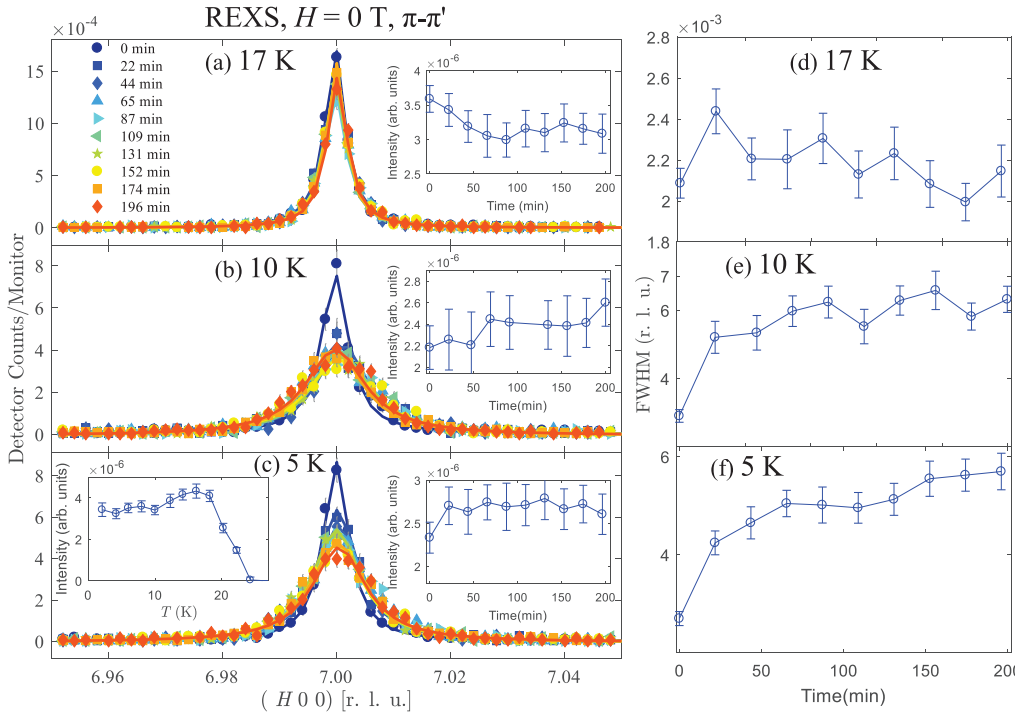

FIG. 2. Temperature and time dependent H-scans around the (7 0 0) reflection in the π-π' channel under a zero external magnetic field at (a) 17 K, (b) 10 K, and (c) 5 K. The solid lines show the fit of a Lorentzian function to the experimental data. Insets (right) of (a)–(c) show the time dependence of the integrated intensity. Inset (left) of (c) shows the temperature dependence of the integrated intensity. (d)–(f) Time dependence of the FWHM at 17 K, 10 K, and 5 K, respectively. The line is a guide to the eye.

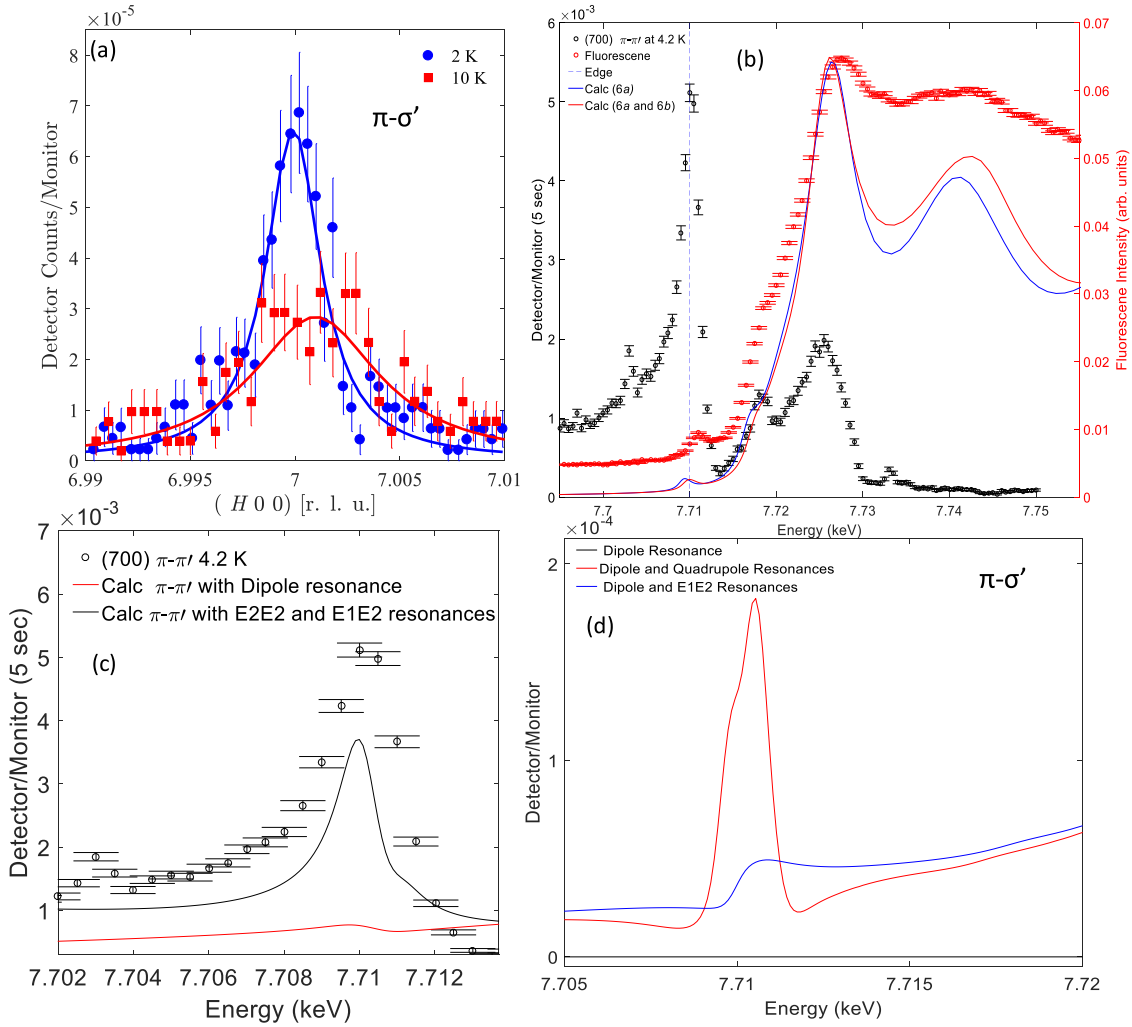

FIG. 3. (a) H-scans around the (7 0 0) reflection in the π-σ' channel at 2 and 10 K. The solid lines are the fit to the data with a Lorentzian function. (b) Energy scan at the (7 0 0) reflection and of the fluorescence signal through the cobalt K-edge. The dashed line indicates the cobalt K-pre-edge. Solid lines represent the calculated XANES spectra using the FDMNES software with contributions from (i) both 6a and 6b sites (red), and (ii) only the 6*a* site (blue). (c) Energy scan at the (7 0 0) reflection (open circles) in the π-π' channel and calculated spectra (black lines), with contributions from quadrupole E2E2 and E1E2 resonances. The red line represents the calculated spectra with E1E1 contributions only. (d) Calculated spectra (considering only 6*a* site) of the energy scan at the (7 0 0) reflection in the π-σ' channel with contributions only from (i) dipole resonance (black line), (ii) dipole and quadrupole resonances (red line), and (iii) dipole and E1E2 resonances (blue line). The calculated spectra with a contribution only from dipole resonance (black line) has been multiplied by 10^{20}.

[Fig. 3(a)]. For moments only along the *c*-axis, the magnetic scattering intensity in the chosen scattering configuration is predicted only in the π-π' channel. Possible reasons for the presence of intensity in the π-σ' channel are (i) the analyzer not being at the optimum position for the photon energy at resonance (leakage), (ii) magnetic moments having an in-plane component, (iii) contributions from dipole-quadrupole, and (iv) quadrupole-quadrupole transitions. The observed intensity in the π-σ' channel is only $\sim$25 times smaller than the intensity in the π-π' channel. This cannot be caused by leakage from the analyzer alone, which for the PG (0 0 6) analyzer at the cobalt K-edge energy is about three orders of magnitude smaller. Since the Co^{3+} ions sit at the inversion center, the dipole-quadrupole contribution, in principle, should be zero. Moreover, at this *Q* location, the dipole-quadrupole contribution should be absent [29]. Allowing the magnetic moment to have an in-plane (*a*-*b*) component contradicts a number of previous observations, where it has already been established that, for the Co^{3+} (TP) ions, the complex d_2 orbital is occupied by the sixth and minority-spin electron (other five electrons have spin-up), which carries a large orbital moment of $2\mu_B$ and generates the Ising-like behavior [42]. This scenario hints at the possibility that the intensity in the π-σ' channel may be related to the quadrupole-quadrupole transition. This is in agreement with previous RXS studies where the observed azimuthal dependence could be described by a combination of E1E1 and E2E2 terms [28]. To confirm the resonance behavior, we performed an energy scan on the magnetic (7 0 0) reflection and compared it with the fluorescence from the sample across the cobalt K-edge [Fig. 3(b)]. A strong resonance enhancement of the (7 0 0) reflection is clearly visible at around 7.710 keV (at the pre-edge), in

addition to two peaks above the edge around energies of 7.717 and 7.725 keV. Theoretical calculations of the cobalt K-edge spectra were performed by carrying out relativistic, spin-polarized, self-consistent field calculations using the FDMNES package [44]. The final electronic states were calculated in a full core-hole screening. Electrical dipolar and quadrupole transitions were considered in the calculations. Atomic clusters inside spheres with a radius of 4.3 Å were considered. The simulations of the x-ray absorption near edge structure (XANES) spectra were carried out using full symmetry calculations in two configurations involving (i) both 6*a* and 6*b* sites, and (ii) only the 6*a* site. The reported magnetic structure [7] was also included in these calculations. Based on the multiple scattering theoretical calculations of the fluorescence spectra, we interpret the peak at 7.710 keV as arising due to the 1*s*-3*d* quadrupole transition. The post-edge peak at 7.717 keV could be due to oxygen-mediated 4*p*-O-3*d* intersite hybridization. In the literature, it has been reported that, due to a mixing of *p* and *d* states over a wide energy range [26], the pre-edge peak has predominant dipole character, which was confirmed experimentally by the twofold symmetry of the azimuthal scan at the (3 2 0) reflection in σ-π' geometry [28]. However, a quadrupole contribution was considered to improve the fit [28]. In our work, the observed intensity of the (7 0 0) reflection in the π-σ' channel is $\sim$3.7% of the intensity in the π-π' channel, which is in agreement with the intrinsic transition strength of the quadrupole transitions and the high density of states of the Co (TP) 3*d*-band. To confirm this further, we carried out simulations of the scattered intensity as function of energy of the (7 0 0) reflection in the π-π' geometry, considering only the 6*a* site [Fig. 3(c)]. It is clear from the simulation results that, at this Q position, a reasonable fit to the energy scans can be obtained by considering only E2E2 and E1E2 contributions. Further, simulations also confirmed that without a contribution from the quadrupole (E2E2) transitions, the intensity in the rotated channel (π-σ' channel) must be negligible [Fig. 3(d)].

In this configuration (horizontal scattering geometry with vertical magnetic field), it is not possible to perform an azimuth scan, which is required to identify the nature of the possible presence of a dipole or higher order moment. Consider this: RXS experiments were carried out in the vertical scattering geometry and the sample was mounted in a Displex closed-cycle cryostat. In the vertical scattering geometry, we measured the azimuth scan on the (3 2 0) reflection, having the same ordering vector as the (7 0 0) reflection. Figure 4 shows the azimuth scan collected in the same resonant condition ($E = 7.710$ keV) in the rotated σ-π' channel at $T = 7.5$ K. Here it may be noted that quadrupole transitions, in principle, can provide information regarding the ordering of both dipole and other higher order moments; however, separating the signal arising from the ordering of magnetic dipole moments is very difficult in the present case as both dipole and quadrupole contributions arise at the same Q vector. In the FDMNES simulations for the azimuth scan (Fig. 4), only the magnetic structure with a dipole magnetic moment along the *c*-axis was considered (E2E2 and E1E2 transitions), and the ordering of the quadrupole (or higher order) moment, if any, was not neglected. The simulation of the azimuth scan in RXS as well

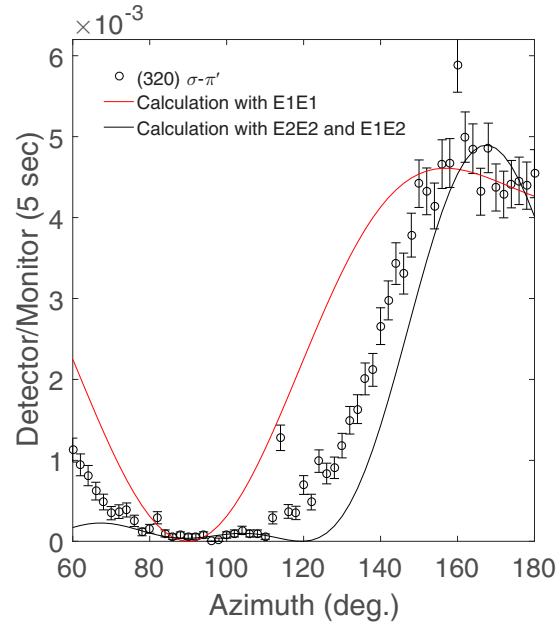

FIG. 4. Azimuth scan (open circled) on the (3 2 0) reflection collected in the rotated σ-π' channel at $T = 7.5$ K. Solid lines are calculated scans considering contributions from (i) E1E1 resonance (red), and (ii) E1E2 and E2E2 resonances (black). The calculations were performed by considering only the ordering of magnetic dipoles, with moment along the *c*-axis.

as the verification of a possible contribution of higher order moments is difficult, especially when the contribution from dipole and other higher order moments appears at the same position in reciprocal space. Nevertheless, the observations of the present study—namely, (i) the flat intensity over a wide range of azimuth angle (80° to 115°), (ii) the inability to fit the observed azimuth scans considering magnetic dipole moments alone, and (iii) the different time and field dependences of the integrated intensity of the magnetic (7 0 0) reflection (compared to reported neutron diffraction data in literature)—suggest the presence of high-order moments. In the literature, using nonresonant inelastic x-ray scattering, it was recently shown that the complex d_2 orbital is stabilized as the lowest energy orbital by the crystal field at the Co (TP) site in $Ca_3Co_2O_6$ [42].

In the following, we investigate the role of a possible involvement of higher order moments in the appearance of the steps observed in the magnetization $M(H)$ [Fig. 5(d), inset (left)]. Figure 5(a) and (b) shows the field dependence of the (7 0 0) peak in the π-π' and π-σ' channels at 10 K, respectively. For both channels, with an increase in the magnetic field, the intensity increases for fields up to $\sim$20 kOe, then decreases sharply and disappears completely at $\sim$40 kOe [Fig. 5, insets (right)]. At 2 K [Fig. 5(c) and (d)], the field dependence of the intensity is similar to that observed at 10 K. The observed increase in intensity for fields up to 20 kOe indicates a transition to a metastable ferrimagnetic (mFIM) state, corresponding to a field-induced magnetization plateau in the $M(H)$ curves [Fig. 5(d), inset (left)]. The (7 0 0) peak disappears for $H \geqslant 40$ kOe, indicating a magnetic field-induced transition to a ferromagnetic phase. This is consistent

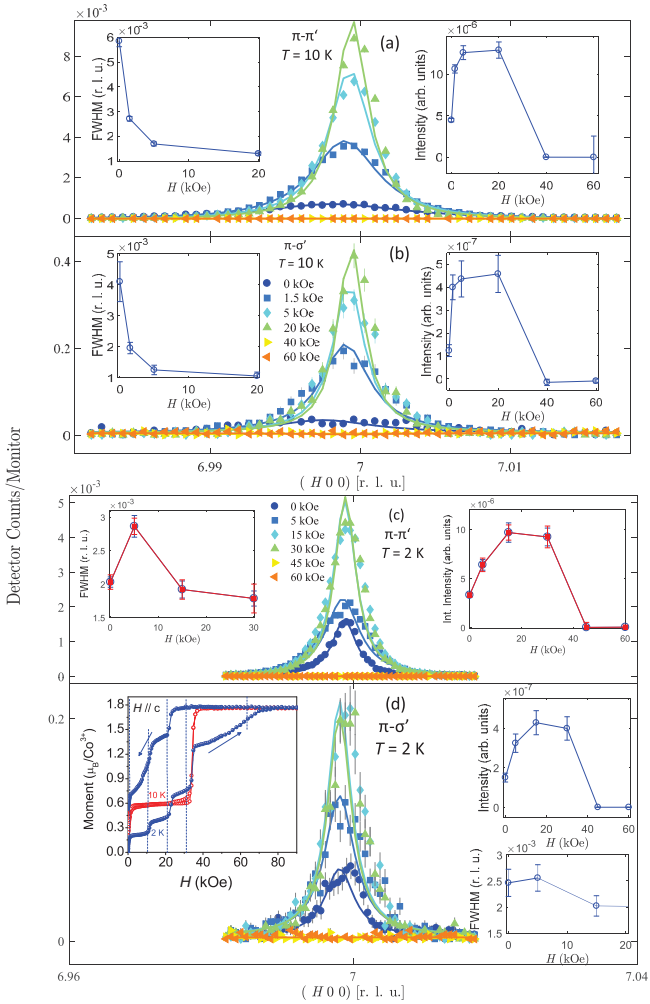

FIG. 5. Magnetic field dependence of the H-scans around the magnetic (7 0 0) reflection measured at (a) 10 K in the π-π' channel, (b) 10 K in the π-σ' channel, (c) 2 K in the π-π' channel, and (d) 2 K in the π-σ' channel. The solid lines are the fit to the experimental data with a Lorentzian function. Insets show the magnetic field dependence of the FWHM and integrated intensity of the magnetic reflection (7 0 0). For these measurements. the sample was cooled from 35 K to the measurement temperatures, and a magnetic field was applied in the increasing direction. Solid circles in the inset of (c) show the magnetic field dependence of the FWHM and integrated intensity with a magnetic field applied in the decreasing direction from 60 to 0 kOe. Solid lines in the insets are guides to the eye. Inset (left) of (d) shows isothermal magnetization at 2 K (solid symbols) and 10 K (open symbols) for magnetic fields applied along the c-axis. The vertical dashed lines show the field-induced transitions. Arrows reveal the directions of field sweeps.

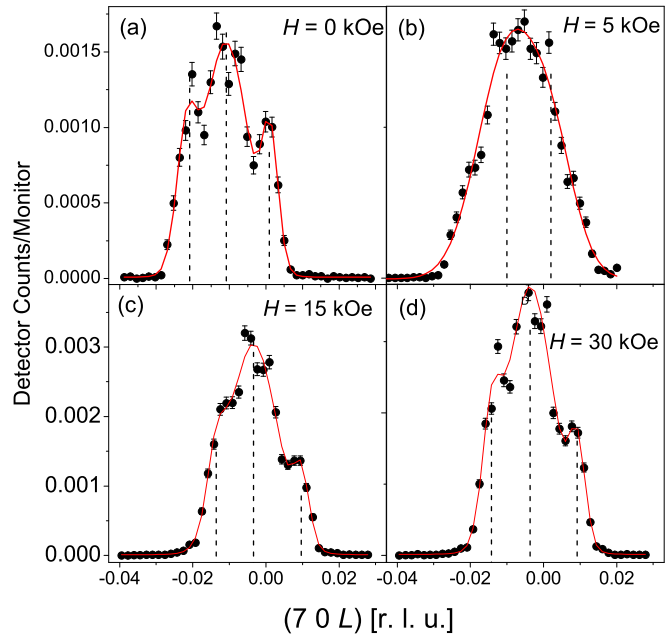

FIG. 6. L-scans around the (7 0 0) reflection in the π-π' channel at 2 K under H = (a) 0, (b) 5, (c) 15, and (d) 30 kOe. The solid lines are the fit to the data with three [two for (b)] Gaussian functions. The vertical dotted lines represent the position of the centers of the Gaussian. For these measurements, the sample was cooled from 35 to 2 K and the magnetic field was applied in the increasing direction. The peak vanishes above $H \geqslant 45$ kOe.

with the field-induced metamagnetic transition at $Hc \sim$ 36 kOe from a ferrimagnetic (spin up-up-down magnetic state) to a ferromagnetic state, observed as a one-third magnetization plateau in the dc magnetization data [Fig. 5(d), inset (left)]. The observed identical behavior for the intensity in the π-π' and π-σ' channels suggests that both have the same physical origin. To investigate the spin correlations at 2 K related to the large hysteresis effects observed in the $M(H)$ curves, [Fig. 5(d), inset (left)], we carried out RXS measurements with increasing (up to 6 T) and decreasing magnetic fields. The most striking feature observed in these measurements is the absence of any hysteresis in the intensity and FWHM of the (7 0 0) reflection in the RXS study [Fig. 5(c), insets]. The observed results in our RXS study are quite different from the reported single-crystal ND results, where a large hysteresis was reported [30]. This observed difference in the field dependent behavior could be due to a contribution from higher order moments.

To investigate the effect of the magnetic field on the spin correlation along the c-axis, we carried out L-scans across (7 0 δ) at 2 K (Fig. 6). The profiles can be fitted by a sum of three (two for 5 kOe) Gaussian functions centered at incommensurate positions for H = 0, 15, and 30 kOe. A shift in the positions of these peaks was observed under applied magnetic fields, indicating that the magnetic field strongly affects the correlation and periodicity of the incommensurate magnetic order along the c-axis. No evidence for the field-induced crystallographic distortions up to 2 T was detected from the θ-scan on the (6 0 0) charge reflection in the π-π' channel, ruling out the possibility of a structural transition (Fig. 7).

We now discuss the difference between the observed time dependence in the present RXS study with those reported in the literature from ND measurements under a zero-applied field [7,8,25,30]. From the single-crystal and powder ND study, it was reported that time dependent magnetic order exists only below ∼13 K, with the dynamics being fastest at 10 K. At 8 K, no change in peak width along (H 0 0) with time was reported by the single-crystal ND study [8]. However, the time variation of the integrated intensity of the

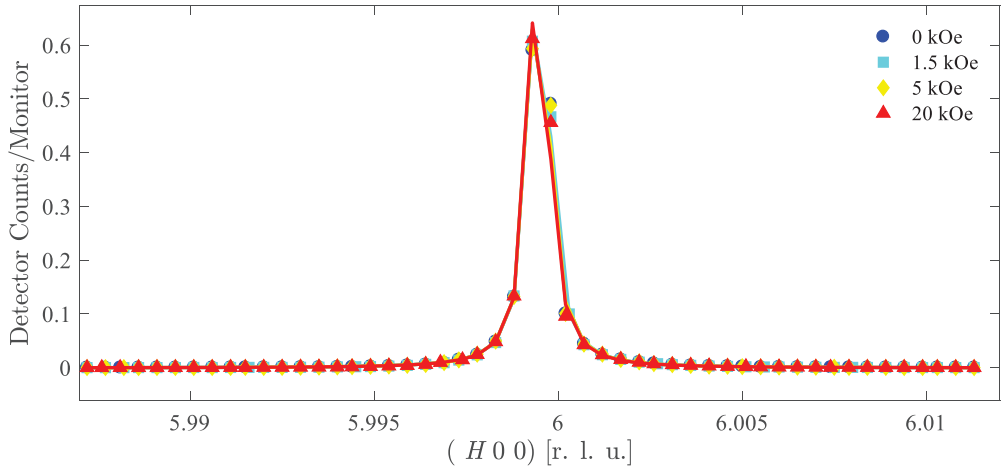

FIG. 7. Magnetic field dependence of the H-scan at the charge Bragg peak (600) in the π-π' channel measured at 10 K. The solid lines are the fit to the experimental data with a Lorentzian function.

(7 0 0) reflection in the present RXS study shows that the time dependent magnetic order is present even at 17 K [Fig. 2(a)]. Moreover, we observe that the peak width also increases with time along the H-scan in the RXS study at 5 K. The observed difference in the dynamics we ascribe to the presence of the higher order moment contribution in the RXS measurements. Here it may be noted that we also observe a quadrupolar moment contribution for the peak at 7.707 keV by the fitting of the azimuthal scan on the (3 2 0) reflection collected in the σ-π'channel. In general, ND senses only dipole magnetic order. The quadrupole moments have no direct interaction with neutron spins and, therefore, are hidden in the ND experiments. Our RXS study suggests the presence of a higher order moment for Co^{3+} ions, which might play a significant role in the observed, fascinating macroscopic behavior of $Ca_3Co_2O_6$ including its dynamics even at 17 K.

Now we discuss the possible origin of time dependent magnetic order. Our recent inelastic neutron scattering study has shown that $Ca_3Co_2O_6$ is highly one-dimensional (1D) in both spin and real space, characterized by a large zone-center gap $(D + J_z)$ of $\sim$27 meV, originating predominately from large single-ion anisotropy D for the Co^{3+} (TP) ions [12]. Here, J_z is the longitudinal component of the exchange interaction. The values of D and J_z cannot be separately extracted for the magnon dispersion. The value of transverse (J_{xy}) components of the magnetic exchange interaction between the neighboring Co^{3+} (TP) ions, which gives rise to the magnon dispersion, is $\sim$0.42 meV. The diffuse magnetic scattering [9], analyzed using the Monte Carlo simulation, has shown that intrachain correlations resemble a ferromagnetic Ising model, with $J_z \sim$ 5 K ($\sim$0.42 meV). This shows that D ($\sim$6.8 meV) is the largest energy scale. From the absence of dispersion perpendicular to the chain, we can put an upper limit of 0.03 meV for the interchain antiferromagnetic interaction (J_{inter}). The lowest energy excitation in this system, therefore, should be a single domain wall (assuming only nearest-neighbor interaction and neglecting the finite, small J_{inter}) with an energy cost $= 2J_zS^2$ (40 K). The domain wall can move easily along the chain with no cost in the energy (if we neglect J_{inter}). Therefore, with the creation of a domain wall, the entropy of the system increases by $k_B \ln N$. Here, N is the number of the possible positions for the domain wall and the resulting free energy cost is $F = 2J_zS^2 – k_BT\log_eN$. This shows that at a finite temperature, the creation of a domain wall will lower the free energy, resulting in the creation of more domain walls until spins are completely randomized. In the literature, the time evolution of the Ising magnets is described using Metropolis dynamics, which in one dimension is called Glauber dynamics [45]. In these 1D Ising magnets, which show no long-range order at a finite temperature, a single spin-flip creates a domain wall that moves along the chain at no energy cost, by a random walk process. The observed slow relaxation of the magnetization in these quasi-1D compounds has been described in terms of domain growth kinetics. It is well established that domain growth as a function of time (t) proceeds as $t^{1/2}$, independent of spatial dimensionality of the system. However, for Ising systems in a geometrically frustrated lattice, the domain growth kinetics become more complicated, as reported for the isosceles triangular Ising antiferromagnet $CoNb_2O_6$ using neutron scattering [46–48]. Here, anisotropic domain growth kinetics has a power-growth law dependence t^n, with $n \sim 0.2$. For the present compound $Ca_3Co_2O_6$, the presence of a small but finite antiferromagnetic interaction J_{inter} coupled with a triangular lattice arrangement of chains gives rise to geometrical frustration, and three-dimensional long-range magnetic order is observed at 25 K. The observed time evolution of the intensity and FWHM of the magnetic (7 0 0) reflection under a zero-applied magnetic field (Fig. 2), and the shift in the position of the (7 0 δ) reflection under small magnetic fields (Fig. 6), indicate the complex nature of the kinetics of the magnetic domains for $Ca_3Co_2O_6$.

The observed time dependent magnetic order for the $Ca_3Co_2O_6$ compound presented here is indeed different from the other compounds of the A_3MXO_6 family. The isostructural compounds Ca_3CoRhO_6 [49,50], Sr_3HoCrO_6 [51], $Ca_3Co_{2-x}Fe_xO_6$, and $Ca_{2.75}R_{0.25}Co_2O_6$ do not show a time dependent magnetic order [14,19,20,22]. The long-time variation in magnetic structure, as observed for the $Ca_3Co_2O_6$ compound, has also been reported for several rare-earth magnetic compounds: $CeIr_3Si_2$, $PrCo_2Si_2$, and $TbNi_2Si_2$ [52]. In $CeIr_3Si_2$, the origin of the long-time variation has been attributed to the slow rate of the nucleation and the growth of a

new magnetic phase due to competing magnetic interactions. However, unlike $Ca_3Co_2O_6$, only the amplitudes of the Bragg peaks are found to vary with time, without any appreciable time variation in the peak position and peak width. Therefore, the results on the compound presented here are unique in every respect with both magnetic correlation lengths and periodicity of magnetic ordering changing.

IV. SUMMARY AND CONCLUSION

In summary, we have carried out single-crystal RXS measurements on the triangular lattice Ising antiferromagnet $Ca_3Co_2O_6$ to probe directly the time, temperature, and magnetic field dependences of the magnetic order. Our simulations of the energy scans, using FDMNES, at the (7 0 0) reflection in the π-π' channel, confirms that a reasonable fit to the energy scans can be obtained by considering only E2E2 and E1E2 contributions. Simulations also confirmed that the intensity in the rotated channel (π-σ' channel) at the (7 0 0) reflection arises due to a quadrupole transition. The observed time evolution of the magnetic (7 0 0) reflection, at 5, 10, and 17 K, under a zero-applied magnetic field, in the π-π' channel, is quite different from the one reported in literature from neutron diffraction studies [8]. In contrast to reported neutron diffraction results, the present RXS study shows no hysteresis in the integrated intensity of the magnetic (7 0 0) reflection for magnetic field increasing and decreasing cycles. The observed flat intensity in the azimuth scan for the magnetic (3 2 0) reflection over a wide angular range (80 ° to 115 °) and the inability to fit the azimuth scans by considering only the ordering of magnetic dipole moments suggest the possibility of the presence of high-order moments for the cobalt ions, probably quadrupole, at the trigonal prism site. Our study further reveals that both in-plane (*a*-*b*) and along the chain, spin-spin correlations are susceptible to the applied magnetic field. It also reveals that the field-induced *Ms*/3 magnetization plateau state corresponds to a mFIM state. With a further increase in the magnetic field, the mFIM state disappears above ∼35 kOe, where a field-induced ferromagnetic state was found in the magnetization study. The observed different dynamics of the magnetic order in our RXS study, compared to the ND study, indicate a different dynamic nature of the dipole and high-order moments. The observed results in the present study will help in understanding the origin of time dependent out-of-equilibrium macroscopic magnetization behavior. These high-order moments might also be responsible for the observed magnetoelectric coupling and high magnetocrystalline anisotropy in $Ca_3Co_2O_6$ and its derivatives [34,41,49–52]

ACKNOWLEDGMENTS

Parts of this research were carried out at the light source PETRA III of DESY. S.M.Y., A.J., and D.K.S. thank the Department of Science and Technology (DST), Government of India, for access to the experimental facility and the financial support to carry out the experiments twice at Deutsches Elektronen-Synchrotron (DESY), Hamburg, Germany under the DST-DESY project. The authors also thank the Saha Institute of Nuclear Physics for managing the project and for beamtime allocation for the proposal (I-20110488). A.J. acknowledges Y. Joly, Institute Neel, CNRS, Grenoble, France for help in simulating the spectra using the FDMNES code.

[1] M. Fruchart, R. Hanai, P. B. Littlewood, and V. Vitelli, Nature (London) **592**, 363 (2021).
[2] J. Demsar, Nat. Phys. **12**, 202(2016).
[3] K. Xu, Z. Sun, W. Liu, Y. Zhang, H. Li, H. Dong, W. Ren, P. Zhang, F. Nori, D. Zheng, H. Fan, and H. Wang, Sci. Adv. **6**, eaba4935 (2020).
[4] P. Högl, T. Frank, K. Zollner, D. Kochan, M. Gmitra, and J. Fabian, Phys. Rev. Lett. **124**, 136403 (2020).
[5] K. R. Beyerlein, Proc. Natl Acad. Sci. USA **115** 2044 (2018).
[6] V. Hardy, D. Flahaut, M. R. Lees, and O. A. Petrenko, Phys. Rev. B **70**, 214439 (2004).
[7] S. Agrestini, C. L. Fleck, L. C. Chapon, C. Mazzoli, A. Bombardi, M. R. Lees, and O. A. Petrenko, Phys. Rev. Lett. **106**, 197204 (2011).
[8] T. Moyoshi and K. Motoya, J. Phys. Soc. Jpn. **80**, 034701 (2011).
[9] J. A. M. Paddison, S. Agrestini, M. R. Lees, C. L. Fleck, P. P. Deen, A. L. Goodwin, J. R. Stewart, and O. A. Petrenko, Phys Rev. B **90**, 014411 (2014).
[10] K. Motoya, T. Kihara, H. Nojiri, Y. Uwatoko, M. Matsuda, and T. Hong, J. Phys. Soc. Jpn. **87**, 114703 (2018).
[11] V. Hardy, M. R. Lees, O. A. Petrenko, D. McK. Paul, D. Flahaut, S. Hébert, and A. Maignan, Phys. Rev. B **70**, 064424 (2004).
[12] A. Jain, P. Y. Portnichenko, H. Jang, G. Jackeli, G. Friemel, A. Ivanov, A. Piovano, S. M. Yusuf, B. Keimer, and D. S. Inosov, Phys. Rev. B **88**, 224403 (2013).
[13] E. V. Sampathkumaran, N. Fujiwara, S. Rayaprol, P. K. Madhu, and Y. Uwatoko, Phys Rev. B **70**, 014437 (2004).
[14] A. Jain, S. Singh, and S. M. Yusuf, Phys. Rev. B **74**, 174419 (2006).
[15] A. Maignan, V. Hardy, S. Hébert, M. Drillon, M. R. Lees, O. Petrenko, D. M. Paul, and D. Khomskii, J. Mater. Chem. **14**, 1231 (2004).
[16] T. Burnus, Z. Hu, M. W. Haverkort, J. C. Cezar, D. Flahaut, V. Hardy, A. Maignan, N. B. Brookes, A. Tanaka, H. H. Hsieh, H.-J. Lin, C. T. Chen, and L. H. Tjeng, Phys. Rev. B **74**, 245111 (2006).
[17] V. Hardy, S. Lambert, M. R. Lees, and D. McK. Paul, Phys. Rev. B **68**, 014424 (2003).
[18] O. A. Petrenko, J. Wooldridge, M. R. Lees, P. Manuel, and V. Hardy, Eur. Phys. J. B **47**, 79 (2005).
[19] A. Jain and S. M. Yusuf, Phys. Rev. B **83**, 184425 (2011).
[20] A. Jain, S. M. Yusuf, J. Campo, and L. Keller, Phys. Rev. B **79**, 184428 (2009).
[21] E. V. Sampathkumaran, Z. Hiroi, S. Rayaprol, and Y. Uwatoko, J. Magn. Magn. Mater. **284**, L7 (2004).

[22] A. Jain, S. M. Yusuf, S. S. Meena, and C. Ritter, Phys. Rev. B **87**, 094411 (2013).
[23] H. Fjellvåg, E. Gulbrandsen, S. Aasland, A. Olsen, and B. C. Hauback, J. Solid State Chem. **124**, 190 (1996).
[24] H. Wu, M. W. Haverkort, Z. Hu, D. I. Khomskii, and L. H. Tjeng, Phys. Rev. Lett. **95**, 186401 (2005).
[25] S. Agrestini, L. C. Chapon, A. Daoud-Aladine, J. Schefer, A. Gukasov, C. Mazzoli, M. R. Lees, and O. A. Petrenko, Phys. Rev. Lett. **101**, 097207 (2008).
[26] R. Frésard, C. Laschinger, T. Kopp, and V. Eyert, Origin of magnetic interactions in $Ca_3Co_2O_6$, Phys. Rev. B **69**, 140405(R) (2004).
[27] H. Kageyama, K. Yoshimura, K. Kosuge, X. Xu, and S. Kawano, J. Phys. Soc. Jpn. **67**, 357 (1998).
[28] S. Agrestini, C. Mazzoli, A. Bombardi, and M. R. Lees, Phys. Rev. B **77**, 140403(R) (2008).
[29] A. Bombardi, C. Mazzoli, S. Agrestini, and M. R. Lees, Phys. Rev. B **78**, 100406(R) (2008).
[30] C. L. Fleck, M. R. Lees, S. Agrestini, G. J. McIntyre, and O. A. Petrenko, EPL **90**, 67006 (2010).
[31] H. Kageyama, K. Yoshimura, K. Kosuge, M. Azuma, M. Takano, H. Mitamura, and T. Goto, J. Phys. Soc. Jpn. **66**, 3996 (1997).
[32] A. Maignan, C. Michel, A. C. Masset, C. Martin, and B. Raveau, Eur. Phys. J. B **15**, 657 (2000).
[33] T. Goko, N. Nomura, S. Takeshita, and J. Arai, J. Magn. Magn. Mater. **272–276**, E633 (2004).
[34] P. Lampen, N. S. Bingham, M. H. Phan, H. Srikanth, H. T. Yi, and S. W. Cheong, Phys. Rev. B **89**, 144414 (2014).
[35] P. Lampen-Kelley, E. M. Clements, B. Casas, M. H. Phan, H. Srikanth, J. Marcin, I. Skorvanek, H. T. Yi, and S. W. Cheong, J. Magn. Magn. Mater. **493**, 165690 (2020).
[36] N. Mohapatra, K. K. Iyer, S. D. Das, B. A. Chalke, S. C. Purandare, and E. V. Sampathkumaran, Phys. Rev. B **79**, 140409(R) (2009).
[37] S. Takeshita, T. Goko, J. Arai, and K. Nishiyama, J. Phys. Chem. Solids **68**, 2174 (2007).
[38] G. Allodi, R. De Renzi, S. Agrestini, C. Mazzoli, and M. R. Lees, Phys. Rev. B **83**, 104408 (2011).
[39] Y. B. Kudasov, Phys. Rev. Lett. **96**, 027212 (2006).
[40] G. Allodi, P. Santini, S. Carretta, S. Agrestini, C. Mazzoli, A. Bombardi, M. R. Lees, and R. De Renzi, Phys. Rev. B **89**, 104401 (2014).
[41] J. W. Kim, E. D. Mun, X. Ding, A. Hansen, M. Jaime, N. Harrison, H. T. Yi, Y. Chai, Y. Sun, S. W. Cheong, and V. S. Zapf, Phys. Rev. B **98**, 024407 (2018).
[42] B. Leedahl, M. Sundermann, A. Amorese, A. Severing, H. Gretarsson, L. Zhang, A. C. Komarek, A. Maignan, M. W. Haverkort, and L. H. Tjeng, Nat. Commun. **10**, 5447 (2019).
[43] N. G. Hegde, I. Levatic, A. Magrez, H. M. Rønnow, and I. Živkovic, Phys. Rev. B **102**, 104418 (2020).
[44] O. Bunau and Y. Joly, J. Phys. Condens. Matter **21**, 345501 (2009).
[45] R. J. Glauber, J. Math. Phys. **4**, 294 (1963).
[46] C. L. Sarkis, S. Säubert, V. Williams, E. S. Choi, T. R. Reeder, H. S. Nair, and K. A. Ross, Phys. Rev. B **104**, 214424 (2021).
[47] S. Kobayashi, S. Mitsuda, T. Jogetsu, J. Miyamoto, H. Katagiri, and K. Kohn, Phys. Rev. B **60**, R9908 (1999).
[48] S. Kobayashi, H. Okano, T. Jogetsu, J. Miyamoto, and S. Mitsuda, Phys. Rev. B **69**, 144430 (2004).
[49] S. Niitaka, K. Yoshimura, K. Kosuge, M. Nishi, and K. Kakurai, Phys. Rev. Lett. **87**, 177202 (2001).
[50] M. Loewenhaupt, W. Schäfer, A. Niazi, and E. V. Sampathkumaran, Europhys. Lett. **63**, 374 (2003).
[51] V. Hardy, C. Martin, G. Martinet, and G. André, Phys. Rev. B **74**, 064413 (2006).
[52] K. Motoya, M. Hagihala, S. Kimura, M. Matsuda, and B. Ouladdiaf, J. Phys. Soc. Jpn. **86**, 034701 (2017).